MRS Advances

Thermoelectric System Economics: Where the Laws of Thermoelectrics, Thermodynamics, Heat Transfer and Economics Intersect

Terry J. Hendricks

Power and Sensors System Section, NASA-Jet Propulsion Laboratory, California Institute of Technology, 4800 Oak Grove Drive, M.S. 277-207, Pasadena, CA 91109

ABSTRACT

Thermoelectric technology has key benefits and strengths in many terrestrial energy recovery applications. Thermoelectric system cost is a key factor governing final decisions on the use of thermoelectric energy recovery systems in all terrestrial applications; thus cost being just as important as power density or efficiency for the adoption of waste energy recovery (WER) thermoelectric generators (TEG). New integrated cost analysis / thermoelectric analysis approaches have now shown key relationships and interdependencies between overall TEG system costs, including TE material costs, manufacturing costs, and specifically heat exchanger costs; and the TE performance design metrics such as TE material properties, TE device design parameters, heat exchanger performance metrics such as hot-side and cold-side conductances and UA values, and hot side heat flux in achieving optimal TEG WER designs. These new approaches have led to a new thermoelectric system economics paradigm that strongly influences TEG cost and performance decisions. While work by Yee et al. and LeBlanc et al. [2, 3] provided foundations for the latest cost scaling analysis / TE performance analysis, this new work takes prior work to new insights and understandings and provides the basis for new thermoelectric system economics. Optimum TEG system cost conditions can now be tied directly to the TE materials, TEG design parameters, and heat exchanger design parameters through critical non-dimensional analysis. The non-dimensional analysis and metrics show the

© 2018 California Institute of Technology. Government sponsorship acknowledged.

TEG system cost and performance interdependencies and interlinks in one unifying and cohesive relationship. Prior work [1, 2] has shown that the system design that minimizes cost (e.g., the G [$/W] value) can be close to designs that maximize power, but these design regimes are not necessarily aligned with high system conversion efficiency or high specific power. This paper will explore the key sensitivities and interrelationships between critical cost metrics and critical TE performance and design metrics in the new thermoelectric system economics paradigm, provide quantitative data showing these sensitivities, and their serious implications on TEG system design in terrestrial WER applications. Critical non-dimensional parameter mapping has shown where heat exchanger cost-dominated conditions, TE material or manufacturing cost-dominated conditions, and combinations of cost conditions control and drive the overall TEG cost and performance. This new cost-performance paradigm shows the required pathways and challenges to achieving TEG system costs of $1-$3/W_{elec}.

INTRODUCTION

Thermoelectric (TE) energy recovery systems worldwide in industrial, automotive, military and spacecraft applications have a common need to demonstrate high performance; as measured by conversion efficiency, power output, power density, or heat or power flux, and low cost to be competitive with various energy conversion technologies. Recent focused attention has been given to cost modeling of cost per watt metrics associated with thermoelectric systems [1-5], in order to evaluate and quantify current cost levels and future potential cost levels for this technology in various energy recovery applications. Comprehensive TE / heat exchanger performance models have been extensively discussed in the literature [6-8]. However, detailed integrated TE/heat exchanger performance – cost analysis models are not readily available or not generally reported on in energy recovery applications. Key system challenges and commercialization barriers are not so much TE performance anymore as they are system-level thermoelectric generator (TEG) costs in energy recovery (ER) applications, such that cost modeling and integrating cost modeling with TEG system-level performance modeling is now critical. LeBlanc et al. [2] and Yee et al. [3] initially investigated cost modeling using simplified TE performance-cost models to get first order estimates of TE system level costs applicable to energy recovery systems. Hendricks et al. [1, 5] followed this work with integration of detailed TE/heat exchanger performance models coupled with the cost modeling to better understand and quantity the cost metrics of real-world TE systems including detailed heat exchanger effects. This work seeks to expand those efforts in seeking a formalized, comprehensive approach that provides a more complete understanding of TE / heat exchanger integration coupled with cost modeling effects. This paper describes detailed thermal / TE system analysis models coupled with the cost modeling work of LeBlanc et al., Yee et al, and Hendricks et al. and new design paradigms resulting from the integrated performance-cost modeling. New relationships are developed from this coupled, integrated TE performance-cost modeling that provide enhanced understanding and elucidate the impacts and interrelationships of optimum TE fill factor, heat exchanger thermal conductance, UAu, and interfacial heat flux in minimizing TEG system costs. The new cost minimization relationships then used to explore the relationships and interdependencies between key TE / heat exchanger design parameters and cost parameters; ultimately leading to new cost regime mapping of heat-exchanger-dominated, TE-materials-dominated, and TE-manufacturing-dominated regimes and their relationships within the overall TEG system design domain for a given ER application.

NOMENCLATURE

English

A_{HEX} – TE/Heat Exchanger Interface Area [m^2]
A_{TE} – Thermoelectric Element Area [m^2]
C_{TEG} – Thermoelectric Generator Cost [$]
C_{HEX} – Heat Exchanger Cost Parameter [$/(W/K)]
C''- TE System Manufacturing/Fabrication Costs per Area [$/$m^2$]
C'''- TE Material Volumetric Costs per Volume [$/$m^3$]
C_p - Exhaust Flow Specific Heat [J/kg-K]
F - Fill Factor
F_{opt} – Optimum Cost Fill Factor
G – Thermoelectric System Cost per Watt [$/W]
I – Thermoelectric Device Current [A]
K_{exh} – Heat Exchanger Conductance [W/K]
K_H – Hot Side Total Thermal Conductance [W/K]
K_C – Cold Side Total Thermal Conductance [W/K]
K_{HX} – Heat Exchanger Conductance Value [W/K]
K_{TE} – Effective Thermoelectric Conductance [W/K]
L – Thermoelectric Element Length [m]
m - Load resistance to TE device resistance ratioTE
$\dot{m}_h$ - exhaust mass flow rate [kg/sec]
N – Number of Thermoelectric Couples
q'' – Thermal Flux [W/m^2]
Q – Thermal Transfer on Hot- or Cold-Side [W]
S_{pn} – Total Seebeck Coefficient (= $S_p + |S_n|$) [V/K]
UA_u – Heat Exchanger UA Value [W/K]
V - Thermoelectric Device Voltage [V]
T – Temperature [K]

Greek

ε - Heat Exchanger Thermal Effectiveness
γ - Thermoelectric Element Length to Area Ratio [m^{-1}]
κ - Thermal Conductivity (thermoelectric material unless otherwise specified) [W/m-K]
η - Thermoelectric Conversion Efficiency
σ - Heat Loss Factor Quantifying Heat Losses (=$Q_{loss}/Q_{h,TE}$) in Eq. 9 or Electrical Conductivity in Eqs. 13, 16 & 18

Subscripts

amb – ambient environment
exh – exhaust conditions
h – associated with TE hot-side parameter
c – associated with TE cold-side parameter
n – associated with TE n-type materials
p – associated with TE p-type materials
TE – Thermoelectric parameter
HEX – Heat Exchanger parameter

THERMAL/THERMOELECTRIC SYSTEM ANALYSIS MODELS

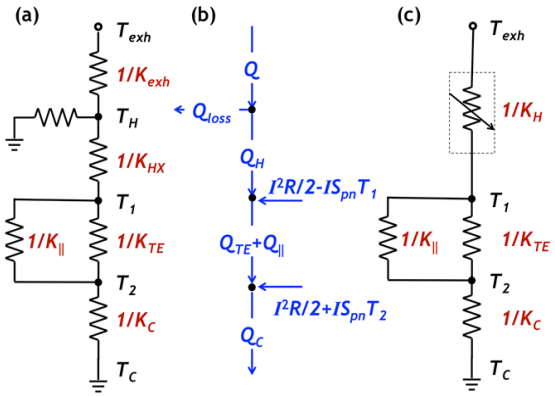

Figure 1 *(a) Thermal resistance network for exhaust heat recovery including leakage from the hot-side heat exchanger. (b) General heat and electrical energy flows. (c) equivalent (traditional) thermal circuit.*

The thermal / TE system modeling starts with the thermoelectric system modeling work of Hendricks and Lustbader [6] and Hendricks and Crane [7] with additional modifications as detailed below and discussed in Hendricks [5]. It is based on the thermal / thermoelectric model shown in Figure 1.

The TE fill factor is standardly defined as:

$$F = \frac{A_{TE}}{A_{HEX}} \qquad (1)$$

at the interface between heat exchanger surfaces and thermoelectric device surfaces. As such, hot-side interfacial thermal energy balance requires that hot-side heat exchanger heat fluxes and hot-side thermoelectric heat fluxes are related through the fill factor:

$$q_{h,HEX} = F \cdot q_{h,TE} = \frac{Q_{h,TE} + Q_{loss}}{A_{HEX}} = f_Q(T_{exh}, T_h, T_c) \qquad (2)$$

In using this relation, one must be very careful to not confuse interfacial heat fluxes with interfacial heat flows. In addition, the fill factor can also be interpreted as "funneling factor", whereby the hot-side thermoelectric heat flux is actually increased over the hot-side heat exchanger heat flux by the "thermal funneling" of heat flow from the heat exchanger into the thermoelectric device. The following Equations 3-8 described the TE voltage - V, current - I, power ($V*I$), hot-side and cold-side thermal flows – Q_h and Q_c respectively, TE element geometry factors - γ_p and γ_n , and TE conversion efficiency relations inherent to this modeling approach. They define the fundamental relationships and linkage between voltage, current, power, thermal flows and conversion efficiency and the TE module geometry, TE fill factor, and heat exchanger interface area, A_{HEX}.

$$\left(\frac{V}{N}\right)^* = f_v(T_h, T_c) \qquad (3)$$

$$(I \cdot \frac{L}{F \cdot A_{HEX}})^* = f_I(T_h, T_c) \tag{4}$$

$$\left(\frac{Q_{h,TE} \cdot L}{N \cdot \mathrm{F} \cdot \mathrm{A_{HEX}}}\right)^* = f_{qh}(T_h, T_c) \tag{5}$$

$$\left(\frac{Q_{c,TE} \cdot L}{N \cdot F \cdot A_{HEX}}\right)^* = f_{qc}(T_h, T_c) \tag{6}$$

$$\left(\frac{\gamma_p}{\gamma_n}\right)^* = f_A(T_h, T_c) \tag{7}$$

$$\eta_{TE}^* = \frac{P}{Q_{h,TE}} = f_{eff}(T_h, T_c) \tag{8}$$

Work by Hendricks et al. [1, 5] has also shown that hot-side thermal transfer is given by:

$$Q_{h,TE} = \frac{(T_{exh} - T_h) \cdot (1 - \sigma_{TE,h})}{\left[\frac{1}{\dot{m}_h \cdot C_p \cdot \varepsilon_h \cdot (1 - \sigma_{HEX,h})} + \frac{1}{K_{HX}}\right]} = K_h (T_{exh} - T_h) \tag{9}$$

and the cold-side thermal transfer is given by a similar expression:

$$Q_{c,TE} = K_c (T_c - T_{amb}) \tag{10}$$

where hot-side heat exchanger effectiveness is defined by:

$$\varepsilon_h = 1 - \exp\left(\frac{-UA_h}{\dot{m}_h \cdot C_p}\right) \tag{11}$$

These equations form a self-consistent set of equations that are functions of hot- and cold-side temperatures and exhaust temperature, as described in Hendricks and Crane [7], that define the complete coupled relationship between the heat exchanger design and the TE device design. The additional terms, TE fill factor, F, and heat exchanger interface area, A_{HEX}, are additional factors to solving these equations, which are tied to this set of performance equations through the additional information in Eq. 2. These equations point out and highlight that the TE fill factor and heat exchanger interfacial area are not "arbitrarily selected" parameters, but instead inherently tied to optimum TE design points at each point in the design space and any desired interfacial heat flux requirements. In most applications, the heat exchanger interface flux, $q_{h,HEX}$, usually has a "target" design value that the application is pursuing to satisfy system volume, weight and/or footprint area requirements. The goal is to use these relationships to determine optimum TE/heat exchanger designs within the overall system design space defined and bounded by the exhaust temperature, T_{exh}, TE hot-side temperature, T_h, TE cold-side temperature, T_c, and ambient temperature, T_{amb}. The complicating factors TE fill factor, interfacial heat fluxes, and the heat exchanger interface area are related by Eq. 2 and provide the ultimate foundation to cost analyses discussed below.

THERMOELECTRIC SYSTEM COST ANALYSIS

The cost analysis leverages work by LeBlanc et al. [2] and Yee et al. [3], with

enhancements as discussed in Hendricks et al. [1]. The total TE system cost is defined by [1, 2, 3]:

$$C_{TEG}[\$] = \left(C''' \cdot L_{TE} + C''\right) \cdot F \cdot A_{HEX} + \left(C_{HEX,h} \cdot K_H + C_{HEX,c} \cdot K_C\right) \tag{12}$$

where the three cost components are volumetric costs associated with TE materials, aerial-related fabrication costs, and heat exchanger costs. Eq. 12 shows that the fill factor, F, and TE device/heat exchanger interfacial heat transfer area, A_{HEX}, is part of what determines system-level TEG costs. When this is considered in concert with the power output generated by the TEG system governed by Eqs. 1-11, which is also dependent on the fill factor and interfacial area, it is clear that the crucial metric cost per watt generated is a complex function of TE device and heat exchanger design parameters and TE device and materials costs and heat exchanger costs. One crucial aspect of terrestrial energy recovery applications is to determine the optimum fill factor that optimally utilizes TE converter and heat exchanger materials and performance to achieve cost and performance goals. Hendricks et al. [5, 9] leveraged the work of Yee et al. [3] and LeBlanc et al. [2] to develop a more rigorous modified relationship for cost per watt, *G*, by eliminating the key assumptions and constraints in Yee et al. [3]:

$$G = \frac{4 \cdot (m+1)^2}{S_{pn}^{\ 2} \cdot \sigma \cdot m \cdot \left(T_{exh} - T_{amb}\right)^2} \cdot \left[\frac{1.1 \cdot \kappa_{TE} \cdot A_{HEX} \cdot F}{K_H} + L_{TE}\right]^2 \cdot \left[C''' + \frac{C''}{L_{TE}} + \frac{C_{HEX} \cdot UA_u}{A_{HEX} \cdot L_{TE} \cdot F}\right] \tag{13}$$

which results when invoking the relationship $K_C \geq 10K_H$ from Hendricks [4]. One goal of this analysis is to determine optimum fill factors, F_{opt}, which minimize the cost function and determine their dependency on heat exchanger conductance, UA_u and interfacial heat flux, q_h''. As discussed by Hendricks et al. [5] this new equation eliminates prior simplifying assumptions and when using this modified cost per watt, *G*, relationship, the $\partial G/\partial F = 0$ condition yields a much more comprehensive and complex relationship for F_{opt}:

$$F_{opt} = \frac{-\left(\frac{\left(C_{HEX,h} + C_{HEX,c}\right) \cdot UA_u}{L_{TE}}\right) \cdot \left(\frac{1.1 \cdot \kappa_{TE}}{K_H}\right) + \sqrt{\left(\frac{\left(C_{HEX,h} + C_{HEX,c}\right) \cdot UA_u}{L_{TE}}\right)^2 \cdot \left(\frac{1.1 \cdot \kappa_{TE}}{K_H}\right)^2 + 8.8 \cdot \left(C''' + C''/L_{TE}\right) \cdot \left(\frac{\kappa_{TE}}{K_H}\right)\left(C_{HEX,h} + C_{HEX,c}\right) \cdot UA_u}}{4.4 \cdot \left(C''' + C''/L_{TE}\right) \cdot \left(\frac{\kappa_{TE} \cdot A_{HEX}}{K_H}\right)} \tag{14}$$

It provides a more accurate representation of the F-dependency on UA_u and interfacial heat flux, $q''_{h,HEX}$, which will be shown below. The terms UA_h and UA_u will be used interchangeably in the following discussions because A_u and A_h are the same in this analysis. Eq. 14 can be mathematically manipulated into a non-dimensional form where F_{opt} is then a function of three key non-dimensional parameters as given by:

$$F_{opt} = -\frac{1}{4} \cdot \left(\frac{\left(C_{HEX,h} + C_{HEX,c}\right) \cdot UA_u}{C''' \cdot L_{TE}^{\ 3} + C'' \cdot L_{TE}^{\ 2}}\right) \cdot \left(\frac{L_{TE}^{\ 2}}{A_{HEX}}\right) + \frac{1}{4}\sqrt{\left(\frac{\left(C_{HEX,h} + C_{HEX,c}\right) \cdot UA_u}{C''' \cdot L_{TE}^{\ 3} + C'' \cdot L_{TE}^{\ 2}}\right)^2 \cdot \left(\frac{L_{TE}^{\ 2}}{A_{HEX}}\right)^2 + \frac{8}{1.1} \cdot \left(\frac{\left(C_{HEX,h} + C_{HEX,c}\right) \cdot UA_u}{C''' \cdot L_{TE}^{\ 3} + C'' \cdot L_{TE}^{\ 2}}\right) \cdot \left(\frac{L_{TE}^{\ 2}}{A_{HEX}}\right)\left(\frac{K_H \cdot L_{TE}}{\kappa_{TE} \cdot A_{HEX}}\right)} \tag{15}$$

This optimum fill factor, F_{opt}, can then be substituted back into G (Eq. 13) to obtain the optimum cost function, G_{opt}, which in turn can be mathematically manipulated to

give a non-dimensional form of the optimum cost function given below:

$$\left[\frac{G_{opt}\left(\frac{\$}{W}\right)\cdot(S\cdot\Delta T)^2\cdot\sigma\cdot L_{TE}\cdot m}{4\cdot\left(C'''\cdot {L_{TE}}^3+C''\cdot {L_{TE}}^2\right)\cdot(m+1)^2}\right] = \left(1+\frac{1.1\cdot\kappa_{TE}\cdot A_{HEX}\cdot F_{opt}}{K_H\cdot L_{TE}}\right)^2 \cdot\left[1+\left(\frac{\left(C_{HEX,h}+C_{HEX,c}\right)\cdot UA_u}{C'''\cdot {L_{TE}}^3+C''\cdot {L_{TE}}^2}\right)\cdot\left(\frac{{L_{TE}}^2}{A_{HEX}\cdot F_{opt}}\right)\right] \tag{16}$$

where $\Delta T = (T_{exh} - T_{amb})$ links the cost impacts to the fundamental overall temperature differential in any given energy recovery application.

Eqs. 15 and 16 show that the optimum TEG cost conditions, F_{opt} and G_{opt}, are functions of three critical non-dimensional parameters:

$$\left(\frac{\left(C_{HEX,h}+C_{HEX,c}\right)\cdot UA_u}{C'''\cdot {L_{TE}}^3+C''\cdot {L_{TE}}^2}\right)$$

$$\left(\frac{{L_{TE}}^2}{A_{HEX}}\right)$$

$$\left(\frac{\kappa_{TE}\cdot A_{HEX}}{K_H\cdot L_{TE}}\right)$$

The first of these is tied to the ratio of heat exchanger costs to TE device costs, the second is coupled to TE device dimensions to TE/heat exchanger interfacial area (basically a geometric factor), and the third is tied directly to TE device/heat exchanger interfacial design parameters and heat exchanger UA_u and heat flux, q_h''. The third term can be shown to be tied directly to the interfacial heat flux, q_h'', by :

$$q_h'' = \frac{K_H\cdot(T_{exh}-T_{hot})}{A_{HEX}} \tag{17}$$

Furthermore, a fundamental TE materials cost parameter (in \$/W) is evident in Eq. 16 defined by:

$$G_o^*\left[\frac{\$}{W}\right] = \frac{4\cdot\left(C'''\cdot {L_{TE}}^3+C''\cdot {L_{TE}}^2\right)\cdot(m+1)^2}{\left(S_{pn}\cdot\Delta T\right)^2\cdot\sigma\cdot L_{TE}\cdot m} = \frac{4\cdot C''\cdot L_{TE}\cdot\left(\frac{C'''\cdot L_{TE}}{C''}+1\right)\cdot(m+1)^2}{(S\cdot\Delta T)^2\cdot\sigma\cdot m} \tag{18}$$

such that G_{opt}/G_o^* is defined by Eq. 16 above, where $\Delta T = (T_{exh} - T_{amb})$ links the cost impacts to the fundamental temperature differential in any given energy recovery application. This strongly shows that energy recovery applications with larger available temperature differentials will have cost advantages and research, development, and deployments should preferably target these. The second form for G_o* reveals a fourth non-dimensional parameter:

$$\left(\frac{C'''\cdot L_{TE}}{C''}+1\right)$$

that can also be extracted from the first two non-dimensional parameters above. This

parameter essentially describes ratio between TE material volumetric costs and TE manufacturing costs and their relative impact on overall TEG system costs. This parameter also is fundamental to determining the relative importance of TE volumetric costs and manufacturing costs and will be discussed further below in mapping out various influential cost regimes.

Yee et al. [3] and LeBlanc et al. [2] originally found a similar, but more restricted, TE cost parameter with a fundamentally different form due to assumptions in their analysis, but this G_o^* is related to all the TE material costs and depicts the fundamental TE material cost per watt. The parameter also contains the fundamental TE material property effects in TEG design, and demonstrating that high power factors generally lead to lower TE material costs per watt and therefore system costs per watt through Eq. 16. The two terms on the right-hand side of Eq. 16 representative multiplicative factors on the fundamental TE materials cost effects elucidated in Eq. 18 and are generally ≥1. Therefore, minimum cost conditions are only achievable when these two terms approach 1. This will be discussed further in section 4.0. Eqs. 15 – 18 therefore define the fundamental overarching relationship between TEG system costs, critical TE materials performance and costs, and heat exchanger performance and costs. Figure 2 shows this non-dimensional cost relationship that defines the entire cost domain for terrestrial TEG systems. Eqs. 15 and 16 most importantly identify and quantify the (F_{opt} , G_{opt}) relationship describing this full cost domain in Figure 2.

CRITICAL LOW TEG COST RELATIONSHIPS

Eq. 15 for F_{opt} has some interesting consequences concerning TE material area to heat exchanger interfacial area that represent a new paradigm compared to common conventional TE device and generator designs. One crucial consequence is that when heat exchanger costs and performance are properly accounted for through $C_{HEX,h}$, $C_{HEX,c}$, UA_u , and interfacial heat flux parameters, then Eq. 15 predicts F_{opt} generally approaching non-traditionally high values of 0.6 to 0.8 when heat exchanger costs are any reasonable value of \$0.5/(W/K) to \$1/(W/K) or higher. Cost-effective, cost-competitive TEG designs require high hot-side-heat-fluxes to help use hot-side conditions most effectively and this manifests itself in higher F_{opt} values. This requirement for high hot-side heat fluxes in TEG systems is similar to that in the solar system designs, where low solar fluxes generally lead to prohibitively high cost systems. This is much higher than common fill factors of 0.15 to 0.2 in conventional TE device designs, which generally derive from manufacturing-related driving factors and considerations and don't necessarily account for heat exchanger costs and performance effects. Interestingly, Eq. 15 does predict optimum fill factors, F_{opt}, near 0.2 when heat exchanger costs are driven artificially low such that they are inconsequential or negligible. High optimum fill factors generally result because a given TEG design must more effectively and efficiently utilize available interfacial heat transfer area and TE device area when heat exchanger costs are significant and non-negligible.

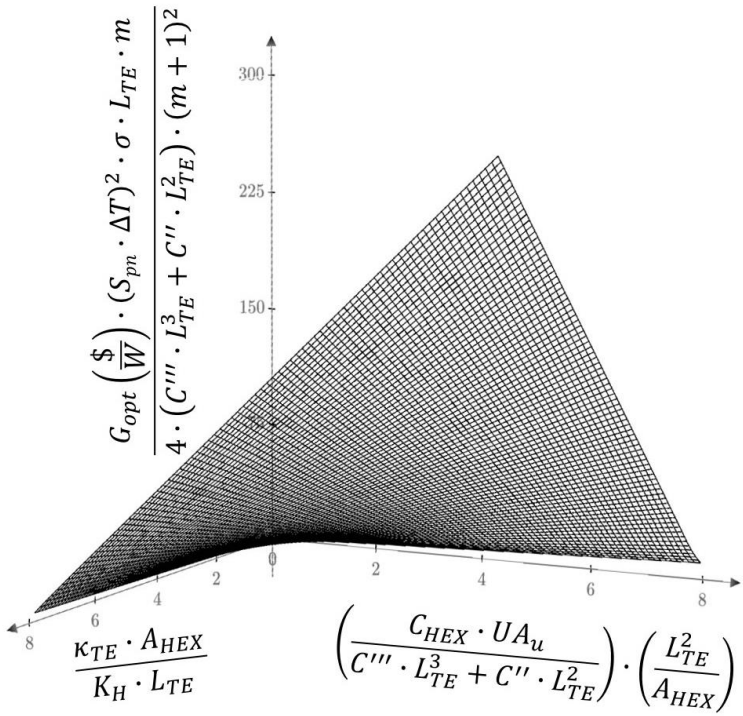

Figure 2. Non-Dimensional TEG Cost Relation Defining Full Cost Domain as Function of Critical Non- Dimensional Parameters - **Intersection of Laws of Thermoelectrics, Heat Transfer, Thermodynamics, and Economics**

Care must be taken in using Eq. 15 for F_{opt} because this equation is developed using merely cost analysis techniques with no accounting for energy conservation or energy balances. Hendricks [9] discusses the constraints, heat flux limits, and proper use of Eq. 15.

Hendricks [9] further observed that two important relationships for minimizing TEG system costs are given by:

$$\left(\frac{\left(C_{HEX,h}+C_{HEX,c}\right)\cdot UA_u}{C'''\cdot L_{TE}^3+C''\cdot L_{TE}^2}\right)\cdot\left(\frac{L_{TE}^2}{A_{HEX}\cdot F_{opt}}\right)<0.05 \tag{19}$$

$$\left(\frac{1.1\cdot\kappa_{TE}\cdot A_{HEX}\cdot F_{opt}}{K_H\cdot L_{TE}}\right)<0.05 \tag{20}$$

This Eq. 19 relationship generally implies that heat exchanger costs must be low and it defines a cost regime boundary for when heat exchanger costs do not dominate the overall TEG system costs. Eq. 20 implies an critically important interface condition between the heat exchanger and TE device. Upon inspection of Eq. 16 if Eq. 19 and Eq. 20 conditions would apply simultaneously, then the overall TEG cost would be controlled primarily by TE material and manufacturing costs.

One final note on Eqs. 19 and Eqs. 20 it is clear how these critical heat fluxes are also dependent on κ_{TE}, L_{TE}, and ($T_{exh} - T_h$). The two parameter κ_{TE} and L_{TE} are TE device design parameters that govern these critical heat fluxes associated with governing and controlling TEG system costs, with lower κ_{TE} and higher L_{TE} both contributing to lower critical cost-driving heat flux levels. This is especially important in offsetting the effects of higher ($T_{exh} - T_h$) to create more power in energy recovery systems when optimizing power output, and lowering cost per watt metrics. This is more evidence of how interrelated and interdependent TE device design, TE material properties, and cost are in TEG energy recovery systems.

These two relationships (Eqs. 19 and 20) can be modified to two other useful forms:

$$\left(\frac{\left(C_{HEX,h} + C_{HEX,c}\right) \cdot UA_u}{C'' \cdot A_{HEX}}\right) < 0.05 \cdot \left(\frac{C''' \cdot L_{TE}}{C''} + 1\right) \cdot F_{opt} \tag{21}$$

$$\left(\frac{\left(C_{HEX,h} + C_{HEX,c}\right) \cdot UA_u}{C'' \cdot A_{HEX}}\right) > \left(\frac{C''' \cdot L_{TE}}{C''} + 1\right) \cdot F_{opt} \tag{22}$$

These two versions show how the earlier TE material cost – TE manufacturing cost parameter

$$\left(\frac{C''' \cdot L_{TE}}{C''} + 1\right)$$

enters into cost regime analysis. One can now use Eqs. 21 and 22 to develop a useful cost regime map to determine some critical influential regions in establishing overall TEG system costs similar to that done by Yee et al. [3]. The important point regarding Eqs. 19 – 22 is that in this integrated cost-performance optimization analysis and process there do evolve crucial relationships between key system design parameters, such interfacial heat flux, $q''_{h,HEX}$, heat exchanger UA_u , A_{HEX} , TE device design parameters, L_{TE} and F_{opt} , and key cost parameters that must be acknowledged and satisfied to minimize cost while maximizing performance.

COST REGIME MAPPING

It is essential and enlightening to determine critical regions where certain costs are dominate in order to understand the entire TEG system cost domain. Equations 21 and 22 allow one to establish a cost regime map defining where heat exchanger, TE materials and TE manufacturing costs will dominate the overall TEG system costs. Figure 3 shows this cost regime map and the critical regions that evolve from Eqs. 21 and 22. This map was first introduced by Hendricks [9], but here it has been expanded to include superimposing constant cost [$/W] lines ranging from ~$1/W to up to $5.60/W onto the map. The cost relationship in Eq. 16 and the two terms on the right-hand side of Eq. 16 will magnify the magnitude of the impacts on overall costs, however the fundamental regime locations from Eqs. 21 and 22 are enlightening. It is clear the impact and influence of F_{opt} in determining and quantifying the key cost regimes in Figure 3 as it is fundamental to setting the regime boundaries. As pointed out in Hendricks [9], F_{opt} will generally be about 0.2 – 0.9 in most energy recovery applications and analyses, such that one can get a sense of where the quantitative boundaries are on the vertical axis of Figure 3 map. An important note is that not only

does this map show the heat-exchanger-dominated, TE-materials-dominated, and TE-manufacturing-dominate regimes, but it also shows the progression from one cost regime to another in formulating the entire oveall TEG system cost picture. The lower Eq. 21 boundary (blue line in Figure 3) show that heat exchangers must be completely neglected or have infinitesimally low costs for TE materials and TE manufacturing to dominate the overall TEG cost picture.

Several illustrative exemplary cost cases are shown in Table 2 using representative cost parameters taken from Hendricks et al. [1, 5] and LeBlanc et al. [2] and ranges in these parameters. Thermoelectric properties and thermoelectric materials costs are taken from Fleurial et al. [10] and other internal Jet Propulsion Laboratory data and internal conversations. These examples cases generally show where common cost parameters and ranges of cost parameters would lie on the cost regime map in Figure 3. It is clear that all of these Table 2 cases are within the heat-exchanger-dominated regime along the $(L_{TE}\ C^{'''}/\ C^{''}) \approx 1$ line. Case C1 approaches a non-heat-exchanger dominated case and if heat exchanger costs were lowered to < \$0.25/ (W/K), then one would approach even closer to the cost regime where TE materials costs, TE manufacturing costs and heat exchanger costs would all contribute significantly to the overall TEG system costs (as shown in Figure 3). This table of example costs was also pointed out by Hendricks et al. [1, 5, 9]. It is also clear in Table 2 that combinations of $C^{'''}$ and $C^{''}$ from Cases A1- C4 could drive these cost regime locations over to the $(L_{TE}\ C^{'''}/\ C^{''}) = 0.1$ line, but still within the heat-exchanger-dominated regime, on the left hand side of Figure 3. Other combinations of $C^{'''}$ and $C^{''}$ between those in Cases A1- C4 can drive $(L_{TE}\ C^{'''}/\ C^{''})$ in between 0.1 and 1.

Table 3 shows additional information for the exemplary cost cases in Table 2 on what typical values for key non-dimensional parameters and G[\$/W] are possible for these heat-exchanger-dominated cases. It is clear from the Table 3 data that $G \sim$ \$3/W or less is only possible when heat exchangers dominate the overall TEG costs and heat exchanger costs are ≤ \$1/W. In this respect heat exchanger costs are critical. It is also clear in Table 3 that it is increasingly difficult to achieve $G <$ \$3/W as TE material and manufacturing costs increase and become more dominant in the overall TEG cost picture. Costs depicted in G begin accelerating as expected when the TE materials and manufacturing costs increase dramatically in Cases C1-C4. This provides a strong argument for the TE community to decrease TE technology (materials and manufacturing) costs as low as possible in order to provide cost-effective, commercializable TEG solutions for terrestrial energy recovery applications. This cost-performance analysis and resulting cost metrics of Cases B2 and B3 in Table 3 also provide reasonable upper bounds to target in the pursuit of cost-effective, commercializable TEG solutions.

Using the technical data in Tables 2 and 3 allows one to locate constant TEG cost [\$/W] lines on the cost regime map as shown in Figure 3. Constant TEG cost lines for three separate heat exchanger cost parameter cases, \$0.25/(W/K), \$1.0/(W/K) and \$2.0/(W/K), are shown and located on the cost regime map in Figure 3. These three heat exchanger cost cases are depicted by the blue, yellow and red lines shown in Figure 3. These constant cost lines are generated by exercising Eqs. 15 and 16 across the parameter space indentified in Figure 3. Constant TEG costs of \$1.01/W, \$0.77/W, and \$0.73/W are established for heat exchanger costs of \$0.25/(W/K), while constant

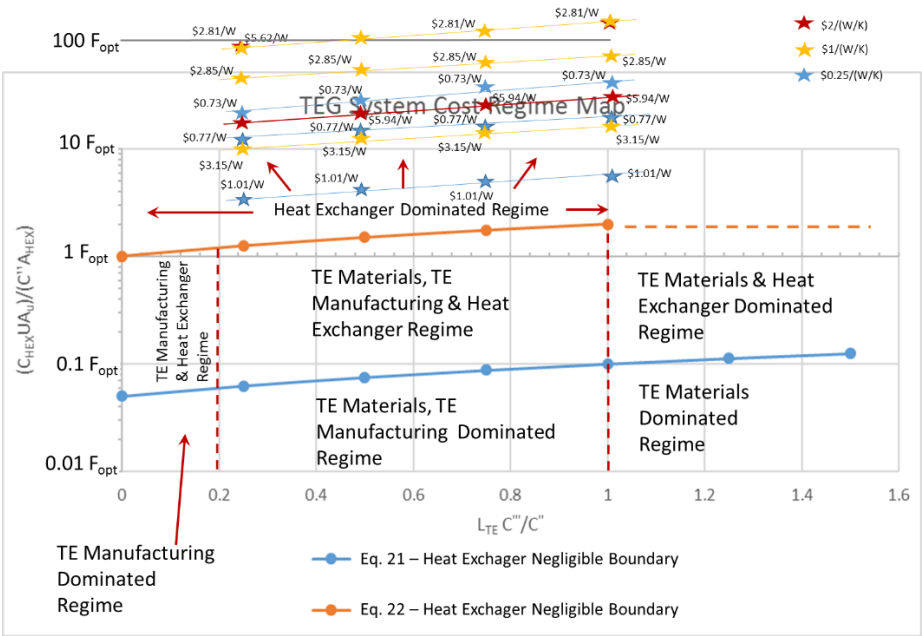

Figure 3 – Cost Regime Map with Constant [$/W] Lines Superimposed on Map. Derived from [9].

Table 2. Exemplary Cost Cases to Demonstrate Key Cost Regime Characteristics & Locations in Figure 3.
Computations use L_{TE} = 0.002 m, κ_{TE} = 2.41 W/m-K, A_{HEX} = 0.0137 m^2 consistent with Jet Propulsion Laboratory TE materials and heat exchanger designs.

	C''' ($/m^3)	C'' ($/m^2)	HEX Costs ($/(W/K))	$\left(\frac{\kappa_{TE} \cdot A_{HEX}}{K_H \cdot L_{TE}}\right)$	$\left(\frac{C_{HEX} \cdot UA_u}{C'' \cdot A_{HEX}}\right)$	$\frac{L_{TE} \cdot C'''}{C''}$
Case A1	8,657x10^4	168.3	$0.25/(W/K)	1.30	22.8	1.02
Case A2	8.657x10^4	168.3	$0.5/(W/K)	1.30	45.5	1.02
Case A3	8.657x10^4	168.3	$1/(W/K)	1.30	91.05	1.02
Case A4	8.657x10^4	168.3	$2/(W/K)	1.30	182.1	1.02
Case B1	2x8.657x10^4	2x168.3	$0.25/(W/K)	1.30	11.4	1.02
Case B2	2x8.657x10^4	2x168.3	$0.5/(W/K)	1.30	22.8	1.02
Case B3	2x8.657x10^4	2x168.3	$1.0/(W/K)	1.30	45.5	1.02
Case B4	2x8.657x10^4	2x168.3	$2.0/(W/K)	1.30	91.05	1.02
Case C1	10x8.657x10^4	10x168.3	$0.25/(W/K)	1.30	2.28	1.02
Case C2	10x8.657x10^4	10x168.3	$0.5/(W/K)	1.30	4.56	1.02
Case C3	10x8.657x10^4	10x168.3	$1.0/(W/K)	1.30	9.11	1.02
Case C4	10x8.657x10^4	10x168.3	$2.0/(W/K)	1.30	18.2	1.02

TEG costs of \$3.15/W, \$2.85/W, and \$2.81/W are demonstrated for heat exchanger costs of \$1/(W/K). It is quite noteworthy that constant TEG cost lines tend to be linear as one traverses across this cost regime map and are approximately parallel to the Eq. 21 heat exchanger domination line in Figure 3. It is very instructive to see that only for the \$0.25/(W/K) heat exchanger cost case (blue lines and stars) do TEG costs achieve \$1.0/W or lower. It is clearly apparent from this data that heat exchanger costs

Table 3. Demonstration of Resulting *G*-Values For the Cost Cases and Cost Regimes in Table 2 - Computations use L_{TE} = 0.002 m, κ_{TE} = 2.41 W/m-K, A_{HEX} = 0.0137 m^2 consistent with Jet Propulsion Laboratory TE materials and heat exchanger designs.

	C''' ($/m^3)	C'' ($/m^2)	HEX Costs ($/(W/K))	$\frac{\kappa_{TE} \cdot A_{HEX}}{K_H \cdot L_{TE}}$	$\left(\frac{C_{HEX} \cdot UA_u}{C''' \cdot L_{TE}^3 + C'' \cdot L_{TE}^2}\right) \cdot \left(\frac{L_{TE}^2}{A_{HEX}}\right)$	G_{opot}/G_o^*	G ($/W)
Case A1	8.657×10^4	168.3	0.25	1.30	11.2	67.79	0.73
Case A2	8.657×10^4	168.3	0.5	1.30	22.43	131.9	1.43
Case A3	8.657×10^4	168.3	1	1.30	44.85	259.9	2.81
Case A4	8.657×10^4	168.3	2	1.30	89.7	515.9	5.58
Case B1	17.31×10^4	2x168.3	0.25	1.30	5.6	35.6	0.77
Case B2	17.31×10^4	2x168.3	0.5	1.30	11.2	67.8	1.47
Case B3	17.31×10^4	2x168.3	1.0	1.30	22.43	131.9	2.85
Case B4	17.31×10^4	2x168.3	2.0	1.30	44.85	259.9	5.62
Case C1	8.657×10^5	10x168.3	0.25	1.30	1.12	9.38	\$1.01
Case C2	8.657×10^5	10x168.3	0.5	1.30	2.24	16.1	1.74
Case C3	8.657×10^5	10x168.3	1.0	1.30	4.49	29.2	3.15
Case C4	8.657×10^5	10x168.3	2.0	1.30	8.97	54.9	5.94

Note: The cost information contained in this document is of a budgetary and planning nature and is intended for informational purposes only. It does not constitute a commitment on the part of JPL and/or Caltech.

must be infinitesimally low for TE materials and manufacturing costs to even begin dominating overall TEG system costs. It is also clear that at all TEG cost conditions from \$1.0/W up to \$5.62/W one is always in the heat exchanger dominated region of the cost map, even when TEG costs are around \$1.0/W, although at this level one is starting to approach the heat exchanger domination boundary. What is keenly interesting is that for a constant heat exchanger cost condition, whether it be \$0.25/(W/K), \$1.0/(W/K) or \$2.0/(W/K), when one progresses from cases C1 to B1 to A1 or C3 to B3 to A3 in Table 3, the TEG system costs go down, but one goes deeper into the heat exchanger dominated region (follow progression of blue and yellow lines). This makes sense because TE materials and manufacturing costs are decreasing strongly in these case transitions. The constant TEG cost lines also indicate that one moves deeper into the heat exchanger dominated region as heat exchanger costs increase, with of course overall TEG costs increasing dramatically as one

progresses from \$0.25/(W/K) to \$2.0/(W/K). This work serves to highlight where many, if not most, TEG system cost cases will reside within the TEG cost regime map.

The major finding here is that, not only does heat exchanger performance impact and govern TEG performance, weight, and volume as discussed in Hendricks et al. [1], heat exchanger are the major cost driver and govern TEG costs for a large portion of the cost regime map.

CONCLUSIONS

This latest work in TE system cost – performance analysis and identification and quantification of cost minimization criteria has uncovered several key relationships for optimum fill factors, interfacial heat flux limits, cost regime boundaries and maps, and highlights how heat exchanger costs impacts and drives TEG system costs. These relationships and cost regime maps provide new TE/heat exchanger design insights and paradigms that can help to guide future TEG system designs toward cost-effective, commercializable TEG solutions in terrestrial energy recovery applications. New interfacial heat flux - cost relationships show that interfacial heat flux must be increased and maximized to the extent possible, while satisfying interfacial energy balances to achieve TEG cost minimization. The dependence of TEG systems costs, G, on heat exchanger performance, UA_u and interfacial heat flux, $q''_{h,HEX}$ have been clearly established in the new (G_{opt}, F_{opt}) relationships, Eqs. 15 and 16, and as well as their dependence on critical non-dimensional design and cost parameters. It is clear that heat exchanger costs dominate the overall TEG system costs relative to TE materials and manufacturing costs in most cases, and this is a necessary condition to even begin bringing overall TEG system costs into the \$3/W range. In addition, it appears that a second necessary condition to achieve the \$3/W TEG cost range is that dominating heat exchanger costs must then be ≤\$1/(W/K). In addition, with heat exchanger costs and interfacial heat fluxes dominating the overall TEG cost picture it is clear that TE/heat exchanger interfacial area becomes an increasingly important and valuable commodity, which drives F_{opt} to much higher than conventional industrial values leading to F_{opt} oftentimes being in the range of 0.6-0.8 to minimize TEG system costs. Cost regime maps have been developed from this cost-performance optimization analysis, complete with superimposed constant TEG cost lines, that delineate the critical heat-exchanger-dominated, TE-materials-dominated, and TE-manufacturing-dominated regimes, along with the intermediate cost regimes that show the progression from one regime to another. Constant TEG cost lines superimposed on the cost regime map establish how the various non-dimensional cost-performance parameters presented and discussed in this work relate to and impact TEG cost relationships. The constant TEG cost lines demonstrate that even at \$1.0/W TEG costs, one is still within heat exchanger dominated regimes. Heat exchanger costs would have to be very small or completely negligible for TEG system costs to be unaffected or driven by them. This work highlights new TEG system design and cost paradigms that have significant implications on future thermoelectric WHR system designs, and their mass, area footprints, volume, performance, and operation.

ACKNOWLEDGEMENTS

This work was carried out under NASA Prime contract NNN12AA01C at the Jet Propulsion Laboratory, California Institute of Technology, under a contract to the National Aeronautics and Space Administration. The author acknowledges Dr. Shannon Yee, George W. Woodruff School of Mechanical Engineering, Georgia Institute of Technology, Atlanta, GA and Dr. Saniya LeBlanc, School of Engineering and Applied Sciences, Department of Mechanical & Aerospace Engineering, George Washington University, Washington, DC for their many enlightening thoughts and conversations in this critical technical area.

References:

[1] Hendricks, T. J., Yee, S. K., and LeBlanc, S., *Journal of Electronic Materials*, 2015, 45, No. 3, 1751-1761, The Minerals, Metals, and Materials Society, Springer, DOI: 10.1007/s11664-015-4201-y.

[2] LeBlanc, S., Yee, S. K., Scullin, M. L., Dames, C., and Goodson, K. E., *Renewable and Sustainable Energy Reviews*, 2014, and 532, 313-327.

[3] Yee, S. K., LeBlanc, S., Goodson, K. E., and Dames, C. *Energy & Environmental Science*, 2013, 6, 2561-2571.

[4] Hendricks, T.J., "Integrated Thermoelectric–Thermal System Resistance Optimization to Maximize Power Output in Thermoelectric Energy Recovery Systems, *Mater. Res. Soc. Symp. Proceedings*, 2014, 1642, Materials Research Society, mrsf13-1642-bb02-04 doi:10.1557/opl.2014.443.

[5] Hendricks, T.J., "Heat Exchanger Performance Impacts on Optimum Cost Conditions in Thermoelectric Energy Recovery Design", 14th European Conference on Thermoelectrics (Lisbon, Portugal), *Journal MaterialsToday: Proceedings*, Vol. 5, Issue 4, Part 1, 10357–10370, Elsevier Ltd., www.sciencedirect.com, Paper # MATPR4597, DOI: 10.1016/j.matpr.2017.12.284, 2017.

[6] Hendricks, T.J. and Lustbader, J. in Proceedings of the 21st International Conference on Thermoelectrics (Long Beach, CA), 2002, IEEE Catalogue #02TH8657, p. 381.

[7] Hendricks, T.J. and Crane, D. "Thermoelectric Energy Recovery Systems: Thermal, Thermoelectric and Structural Considerations", **CRC Press Handbook of Thermoelectrics & Its Energy Harvesting: Modules, Systems, and Applications in Energy Harvesting**, Book 2, Section 3, Chapter 22, Taylor and Francis Group, Boca Raton, FL, 2012.

[8] Crane, DT and LE Bell, 2009, "Design to Maximize Performance of a Thermoelectric Power Generator With a Dynamic Thermal Power Source," *Journal of Energy Resources Technology*, 131:012401-1 to 8.

[9] Hendricks, T.J., "New Paradigms in Cost Optimization of Thermoelectric Energy Recovery Systems", 15th European Conference of Thermoelectric (Padova, Italy), *Journal MaterialsToday:Proceedings*, Elsevier Ltd., www.sciencedirect.com, 2018. Paper accepted and in publication .

[10] J.-P. Fleurial, S.K. Bux, B.C.-Y. Li, S. Firdosy, N.R. Keyawa, P.K. Gogna, D.J. King, J.M. Ma, K. Star, A. Zevalkink, and T. Caillat, in Symposium BB: thermoelectric materials–from basic science to applications, Proceedings of 2013 Materials Research Society Fall Meeting, Boston (2013).